Antarct. Meteorite Res., **17**, 35–54, 2004

Petrology of the Yamato 980459 shergottite

Yukio Ikeda

Department of Materials and Biological Sciences, Ibaraki University, Mito 310-8512
E-mail: y-ikeda@mx.ibaraki.ac.jp

(Received March 2, 2004; Accepted May 21, 2004)

Abstract: Y980459 is a new type of shergottite, consisting mainly of olivine, orthopyroxene with augite mantles, and glassy groundmass. The constituent minerals crystallized under a rapid cooling condition. The cores of olivine phenocrysts are Fo_{85-73}, and Fo_{85} is the most magnesian composition among all martian meteorites. The magnesian olivine may be mostly phenocrysts which crystallized from the parent magma having the Y980459 bulk composition. Many magmatic inclusions occur in olivine phenocrysts around Fo_{74}. They consist mainly of glass, and the trapped melt composition was estimated from the inclusion glass by addition of the wall olivine. The trapped melt represents the early- to middle-stage melt of the Y980459 crystallization sequence. The cores of pyroxene are orthopyroxene, which are surrounded by augite mantles showing remarkable normal zoning. The glassy groundmass contains quenched crystals of ferroan olivine and clinopyroxenes set in a glassy groundmass. Shock-melt pockets occur in Y980459, and the shock degree, which was originally defined for ordinary chondrites (D. Stöffler *et al*.; Geochim. Cosmochim. Acta, **55**, 3845, 1991), corresponds to S3 for Y980459. A new stage classification for lithological types of the shergottite group is proposed, and the Y980459 meteorite is classified as an olivine-bearing glassy basaltic type.

key words: Martian meteorites, olivine-phyric shergottites, glassy basaltic type, Y980459, magmatic inclusions

1. Introduction

Martian meteorites (SNC meteorites and ALH84001 meteorite) are considered to originate from Mars (McSween, 1994). Among them, basaltic and olivine(Ol)-phyric shergottites represent martian magmas, although they seem to contain more or less cumulus phases or xenocrysts (McSween and Jarosewich, 1983; Hale *et al*., 1999; Goodrich, 2003). Shergottites consist mainly of pyroxene and maskelynite with variable amounts of olivines, and the group was further classified into two subgroups, basaltic and lherzolitic (McSween,1994). The maskelynite was produced from plagioclases by impact shocks (Stöffler, 2000), which expelled the meteorite from Mars. However, in case that the shock metamorphism was too intense, the plagioclases in the martian rocks were melted, and then the melt was quenched as plagioclase-glass in the interplanetary space. Some shergottites contain plagioclase-glass instead of maskelynite (Ikeda, 1994, 1997; Ikeda *et al*., 2002), indicating that shergottites could be defined as a group

containing maskelynite or plagioclase-glass. The basaltic shergottites were further grouped into two types, basaltic and Ol-phyric (Goodrich, 2002).

Recently a new Ol-phyric shergottite, Y980459, was recovered from the Antarctica (Kojima and Imae, 2002). It consists mainly of olivine, pyroxenes, and glassy groundmass with minor chromite and sulfide, and neither contains maskelynite nor plagioclase-glass, suggesting that it could not be classified as a shergottite. However, Y980459 has a bulk chemical composition similar to other Ol-phyric shergottites (Dreibus *et al*., 2003; Shih *et al*., 2003), indicating that it should be chemically classified as an Ol-phyric shergottite. Therefore, we need a new definition for "shergottites including the glassy basaltic shergottite".

Y980459 is now studied by a consortium (Misawa, 2003), and this paper is one of the consortium studies, covering the petrology of the meteorite. The petrology and mineralogy of the new shergottite, the crystallization of the meteorite, and a new definition for lithological types of shergottites will be discussed in this paper. Some olivine grains in the meteorite contain many magmatic inclusions, and their origin will be also discussed.

2. Analytical method

Major element compositions of the constituent minerals and glass were analyzed, using an electron-probe micro-analyzer (EPMA, JEOL733 type). A sample current of 5–10 nA, accelerating voltage of 15 kV, and measuring time of 10 s for a peak and background were adopted, while a sample current of 3 nA was used for glass to avoid evaporation loss of alkalis. The corrections were carried out by the Bence and Albee method for silicates and oxides, and the standard ZAF method for sulfides. The groundmass contains needle-like quenched crystals in groundmass glass, and the chemical composition of the bulk groundmass including the quenched crystals and glass was analyzed by a broad beam of EPMA with a 50 μm diameter. The special correction for the broad beam method was not applied because the most quenched crystals are so small with the width less than a few μm.

The modal composition was obtained for the Y980459 lithology by measuring the point percents of the constituent phases using a focused beam of EPMA. The total number of points was 3000 for a thin section.

3. Petrography

3.1. Texture and constituent minerals

Texture of Y980459 is vitrophyric with olivine and pyroxene grains (Fig. 1a,b,c,d). The olivines occur as phenocrysts or microphenocrysts with their width less than 1 mm (Fig. 1c). Greshake *et al*. (2003) showed a bimodal grain size distribution of olivine with a small grain size (30–350 μ) and a large grain size (600–1150 μ). Olivine just in contact with groundmass glass has a ferroan rim with width less than 10 μm (Fig. 1e). Cores of olivine phenocrysts are magnesian, and sometimes discontinuous zoning is observed in the cores (Fig. 1f). The olivine grains seem to have weak alignment due to preferred orientation of olivine grains. The pyroxenes occur as microphenocrysts, and

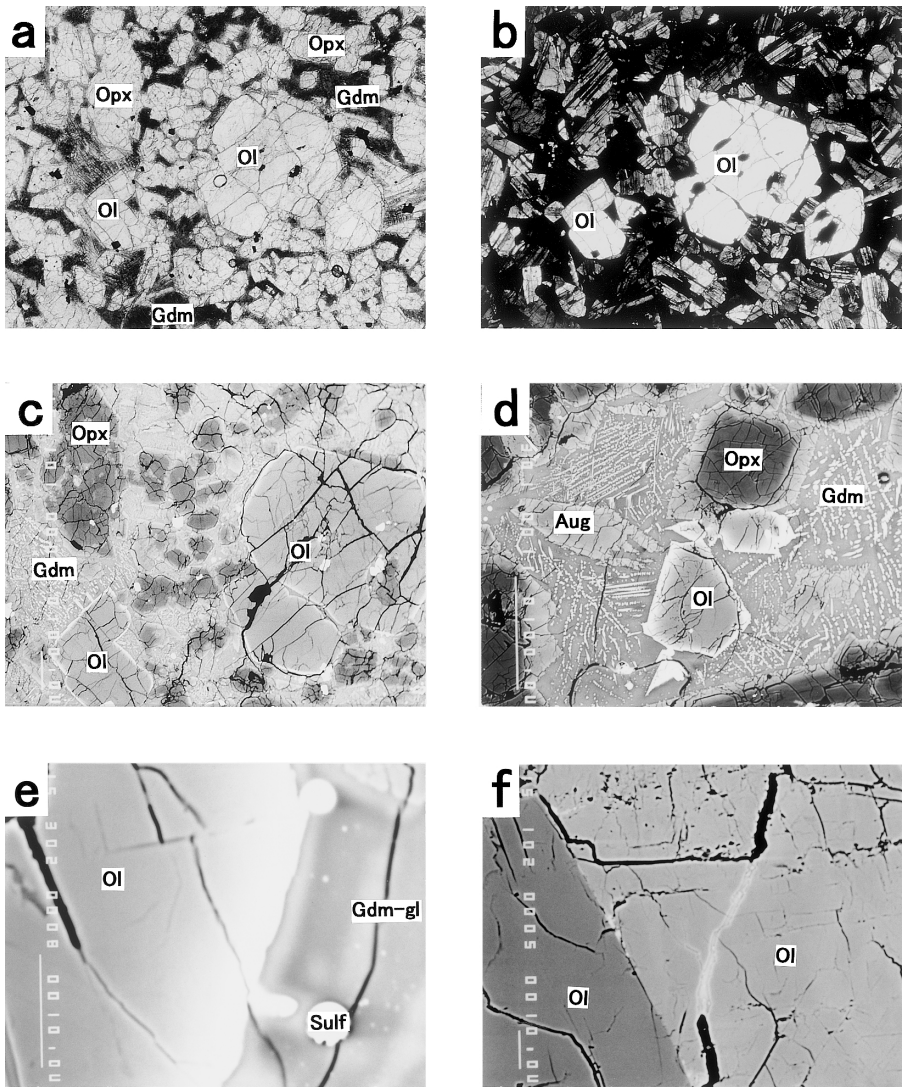

Fig. 1. Photomicrographs (a & b) and back-scattered electron (BSE) images (c–l) of the Y980459 shergottite.

(a) Porphyritic lithology of Y980459. Abbreviation; olivine (Ol), orthopyroxene (Opx), and groundmass (Gdm). Width is 1.76 mm. Open Nicol.

(b) The same figure as (a). Crossed Nicol.

(c) Enlarged BSE image of (a) with phenocrystic olivine (Ol) and microphenocrystic orthopyroxene (Opx) in glassy groundmass (Gdm). Width is 1.12 mm.

(d) Olivine shows chemical zoning from magnesian cores to ferroan rims, orthopyroxene has augite mantle, and augite (Aug) occurs in glassy groundmass. Width is 380 μm.

(e) Olivine has a ferroan rim just in contact with the groundmass glass (Gdm-gl). Sulfide spherules (Sulf) occur in groundmass glass. Width is 38 μm.

(f) Inside of an olivine phenocryst showing a sharp boundary between dark olivine ($Fo_{83–85}$) and gray olivine ($Fo_{79–80}$), suggesting that Mg-Fe diffusion did not take place in the olivine phenocryst. Width is 112 μm.

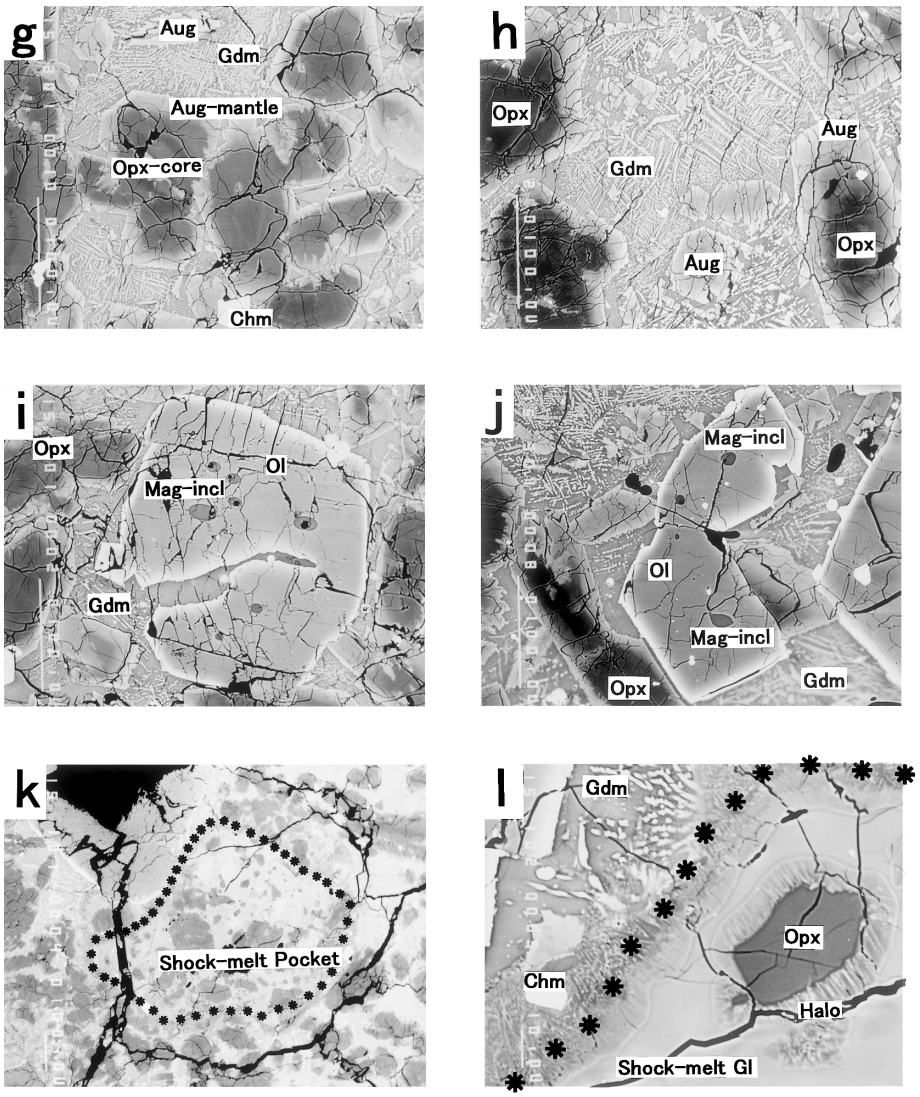

Fig. 1 (continued).

(g) Orthopyroxene core (Opx-core) and augite mantle (Augite-mantle) in glassy groundmass. Chromite (Chm). Width is 380 μm.

(h) Glassy groundmass containing many dendritic crystals in the groundmass glass. A white small grain in an orthopyroxene grain (right) is chromite. Width is 380 μm.

(i) and (j) Magmatic inclusions (Mag-incl) in olivine phenocrysts. These inclusions consist of clean glass. Width is 380 μm.

(k) A shock-melt pocket is surrounded by asterisks. Width is 1.12 mm.

(l) Enlarged BSE image of (k). Boundary between the shock-melt pocket of (k) and the host lithology (upper left) is shown by asterisks. A relic orthopyroxene grain in shock-melt glass (shock-melt Gl) is surrounded by a halo (Halo). Width is 112 μm.

most of the pyroxene grains are rectangular in shape and smaller than 550 μm in length and 270 μm in width (Fig. 1c,d). The groundmass is glassy with many quenched crystals (Fig. 1d). The quenched groundmass crystals are needle-like dendritic grains of ferroan olivine and fine-grained Al-rich clinopyroxenes, which are set in the brownish clean glass of the groundmass (Fig. 1d). Accessory minerals are chromite and sulfide. Chromite occurs in olivine, pyroxene and groundmass, and its sizes are smaller than 150 μm (Fig. 1g,h). Sulfide is pyrrhotite with a spherical shape and diameters smaller than 20 μm, and it occurs in groundmass glass (Fig. 1e). Magmatic inclusions are included in olivine phenocrysts (Fig. 1i,j). Y980459 contains shock-melt pockets (Fig. 1k) and minor shock veins.

3.2. Modal composition

The modal composition of the Y980459 shergottite is olivine (8.7 vol%), low-Ca pyroxene (35.3%), augite (17.4%), glassy groundmass (37.4%), chromite (0.7%), and pyrrhotite (0.4%). There is no maskelynite or plagioclase-glass. Phosphate also does not occur in Y980459, although phosphates always occur in other shergottites. The modal composition of Y980459 obtained by Greshake *et al*. (2003) is olivine (15.7%), clinopyroxene (24.7%), orthopyroxene (27.9%), groundmass (30.9%), chromite (0.5 %), sulfide (0.35%), and melt inclusions (0.1%). The modal compositions for a thin section of the meteorite seem to be slightly different from each other.

3.3. Magmatic inclusions

The olivine phenocrysts in Y980459 sometimes contain magmatic inclusions (Fig. 1i,j). Their shapes are rounded to elliptic with diameters smaller than 100 μm. The magmatic inclusions consist mainly of glass, but rarely contain feathery crystallites. Magmatic inclusions are not yet found in pyroxene grains in the used thin section of Y980459.

The groundmass glass of Y980459 is rarely engulfed into some olivine phenocrysts (Fig. 1i). The perpendicular cutting planes of the engulfed groundmass glass gives ellipsoidal appearance under a microscope, which are similar to the magmatic inclusions in olivine phenocrysts. Magmatic inclusions are always surrounded by magnesian olivines around Fo_{74}, but the engulfed groundmass glass always surrounded by more ferroan olivines.

Magmatic inclusions are common in other martian meteorites. They occur in olivine and rarely pyroxene. Usually they are surrounded by pyroxene mantles, and the cores of inclusions consist mainly of needle pyroxene grains and glass with or without plagioclase or amphibole (Floran *et al*., 1978; Harvey and McSween, 1992; Treiman, 1985; Ikeda, 1998). The mineral assemblages of magmatic inclusions in many martian meteorites other than Y980459 decidedly differ from the glassy nature of magmatic inclusions in Y980459.

3.4. Shock-melt pockets

Shock-melt pockets occur in Y980459 (Fig. 1k,l), and they consist mainly of shock-melt glass, relic olivine, relic orthopyroxene, and relic chromite. The relic orthopyroxene grains are always surrounded by halos (Fig. 1l), although relic olivine

and chromite are not. The halos have chemical compositions corresponding to the mixtures of orthopyroxene with minor shock-melt glass. The averaged composition of the shock-melt glass is shown in Table 2.

4. Mineralogy

4.1. Olivine

The olivine phenocrysts show normal zoning from magnesian cores with Mg/(Mg +Fe) atomic ratios (mg) of 0.85–0.73 to ferroan rims with mg=0.70–0.30 (Table 1). The width of the ferroan rims is less than about 10μm (Fig. 1d,e). Dendritic ferroan olivines with mg ratios from 0.35 to 0.15 occur in the groundmass. The minor components (MnO, Cr_2O_3, CaO) of olivines are shown in Fig. 2. The MnO and CaO contents of olivines increase with the Fe/(Mg+Fe) atomic rations (fe ratios), although the Cr_2O_3 contents rapidly decrease from 0.5 wr% to less than 0.1 wr%. The compositional range of fe ratios for Y980459 olivines is shown in Fig. 3 in comparison to those of other martian meteorites. Olivines in Y980459 are the most magnesian among all martian meteorites.

4.2. Pyroxenes

The pyroxene grains show compositional zoning from magnesian orthopyroxene cores with mg=0.83–0.74 to ferroan augite mantles with mg=0.70–0.30 (Fig.1g,h). Fine-grained ferroan pigeonite and augite with mg ratios from 0.6 to 0.2 occur in the groundmass, and they are enriched in Al_2O_3 (Table 1). Figure 4 shows the Ca-Mg-Fe atomic ratios of pyroxenes, where pyroxene cores are low-Ca orthopyroxene showing slight normal zoning. The mantle augite is more ferroan than the core orthopyroxene, showing remarkable normal zoning. The boundary between core orthopyroxene and mantle augite is unclear; the orthopyroxene rapidly changes to augite in a short distance, although the Becke's line is not observed under a microscope. Mikouchi *et al*. (2003) presented continuous zoning from orthopyroxene to augite *via* pigeonite. The chemical compositions of averaged orthopyroxene and averaged augite are shown in Table 1. As

Table 1. Averaged chemical compositions of core & rim olivines, averaged orthopyroxene (av.Opx), averaged mantle-augite (av.Aug), averaged pyroxene (av.Pyx=2av.Opx+1av.Aug), groundmass pigeonite (Gdm Pig) & augite (Gdm Aug), core & rim chromites (Chm), and pyrrhotite (Pyrrh).

	core Ol	rim Ol	av.Opx	av.Aug	av.Pyx	Gdm Pig	Gdm Aug	core Chm	rim Chm	Pyrrh	
SiO_2	39.89	34.52	55.23	49.61	53.36	45.95	43.51	0.00	0.00	S	36.96
TiO_2	0.00	0.01	0.02	0.68	0.24	0.98	2.48	0.44	0.73	Cr	0.01
Al_2O_3	0.00	0.06	0.44	4.08	1.65	6.86	10.23	5.69	8.84	Fe	58.04
Cr_2O_3	0.42	0.00	0.55	0.38	0.49	0.00	0.00	61.18	57.49	Co	0.24
FeO	14.68	49.28	13.69	17.04	14.81	28.33	23.98	23.93	27.14	Ni	2.18
MnO	0.26	0.83	0.44	0.55	0.48	0.69	0.53	0.24	0.27	Total	97.43
MgO	44.24	14.77	27.13	12.85	22.37	9.28	4.11	7.17	5.93		
CaO	0.11	0.52	1.82	13.89	5.84	8.45	13.75	0.00	0.02		
Na_2O	0.00	0.05	0.03	0.10	0.05	0.07	0.38	0.02	0.00		
K_2O	0.00	0.00	0.00	0.00	0.00	0.00	0.00	0.00	0.00		
P_2O_5	-		-	-	-			-			
Total	99.62	100.03	99.35	99.18	99.29	100.61	98.97	98.69	100.46		
mg	0.84	0.35	0.78	0.58	0.73	0.37	0.23	0.35	0.28		

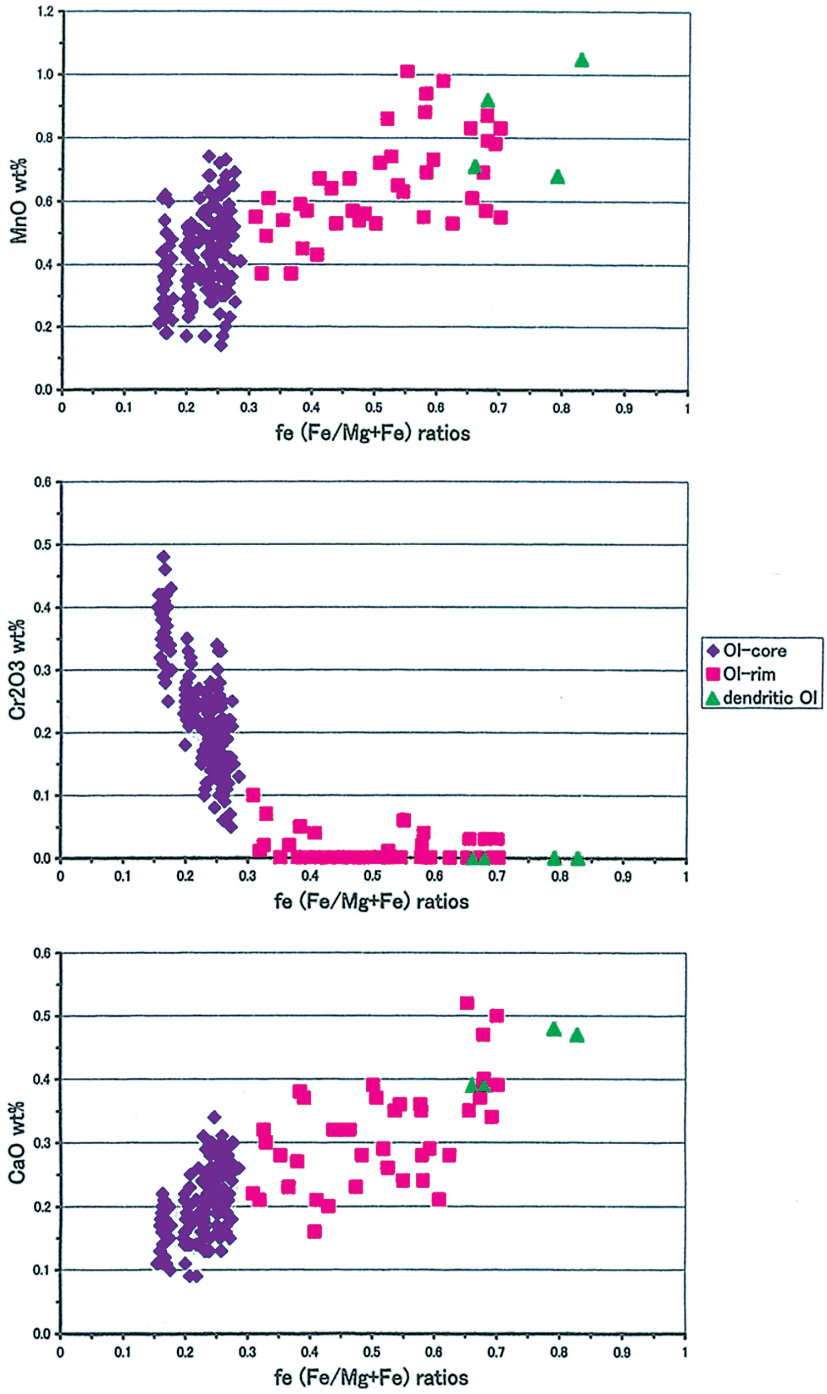

Fig. 2. Minor element contents (MnO, Cr_2O_3, CaO) of olivine are plotted against their fe ratios (Fe/Mg+Fe atomic ratios).

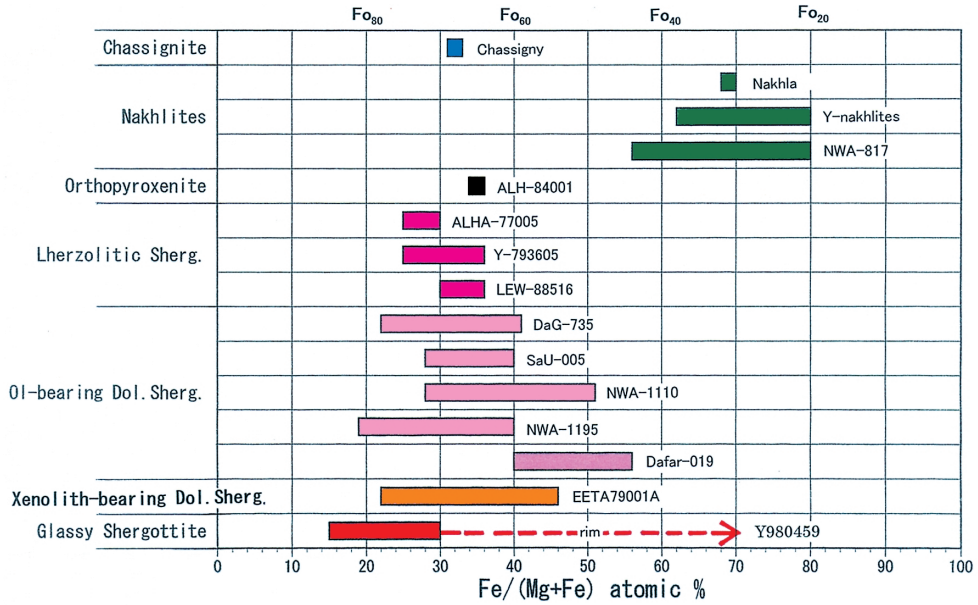

Fig. 3. Compositional ranges of olivines in martian meteorites. The ranges of olivine in Y980459 are very wide, and the rims zone to ferroan olivine which is shown by an arrow. Data source: Floran et al., 1978; Bunch and Reid, 1975; Imae et al., 2003; Sautter et al., 2002; Harvey and McSween, 1994; Ikeda, 1994, 1997, unpublished data; Russell et al., 2002, 2003; Mikouchi and Miyamoto, 2002; McSween and Jarosewich, 1983.

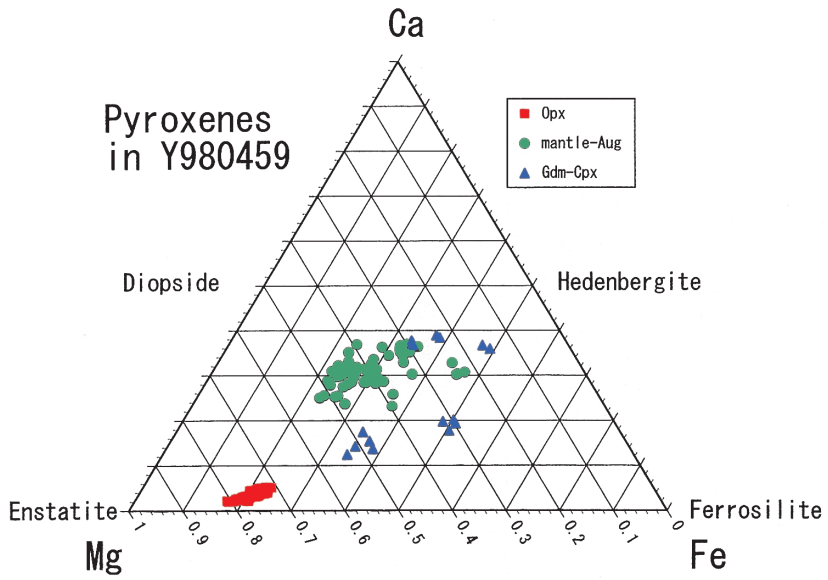

Fig. 4. Pyroxenes in Y980459 are plotted in atomic ratios of Ca, Mg, and Fe.

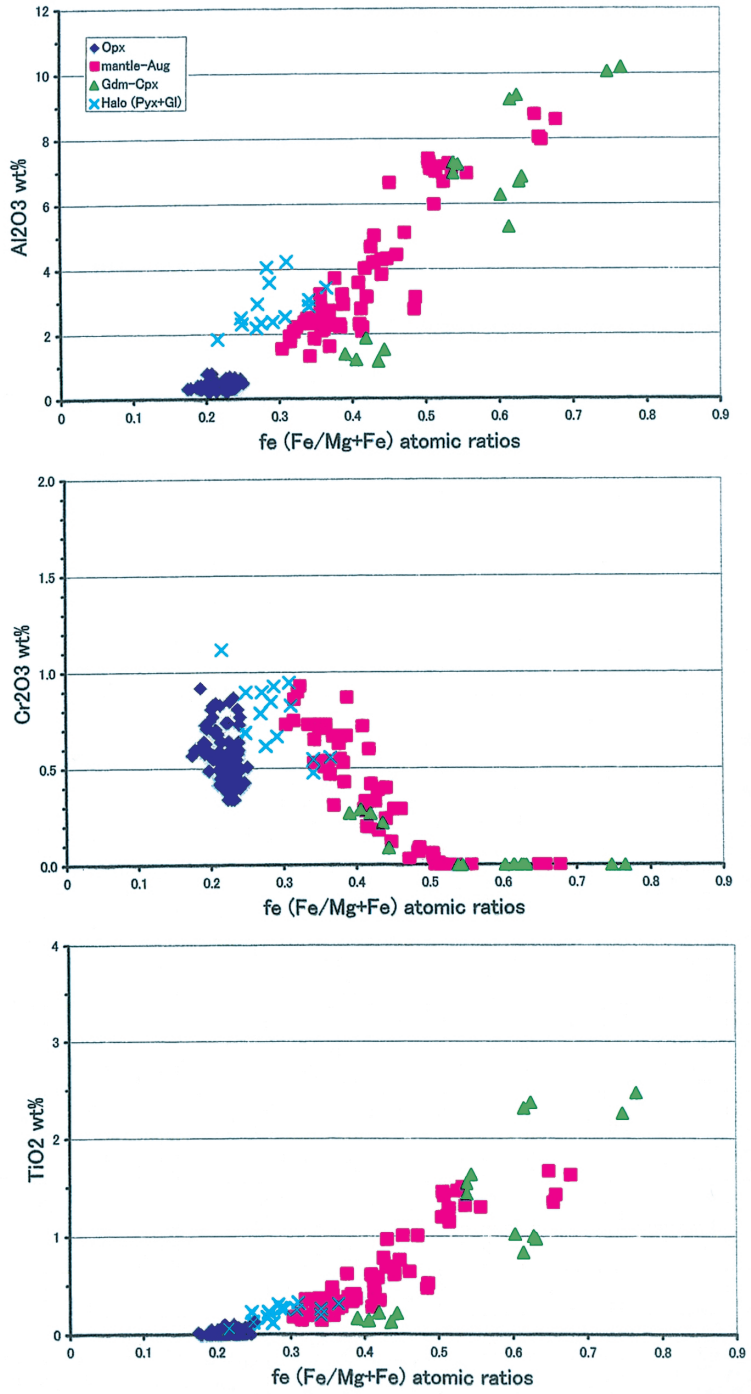

Fig. 5. *Minor element contents* (Al_2O_3, Cr_2O_3, TiO_2) of pyroxenes in Y980459 are plotted against their fe ratios.

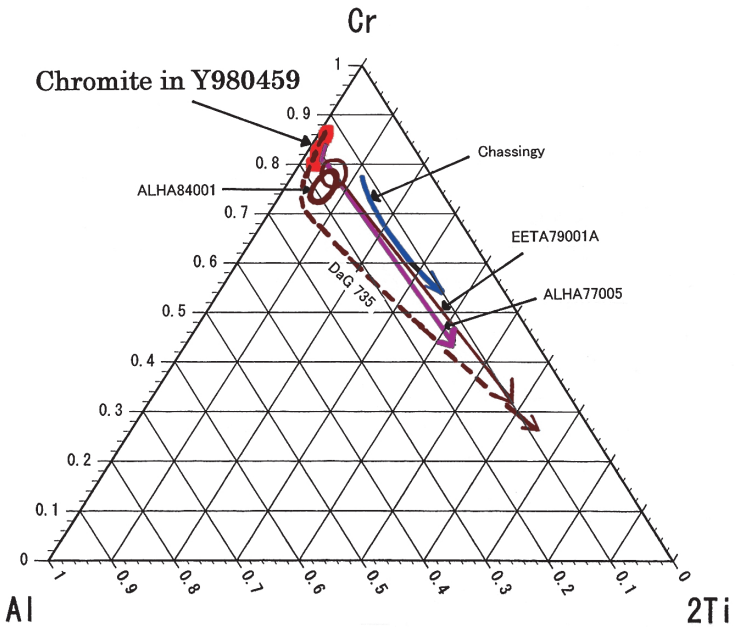

Fig. 6. Chromites in Y980459 are plotted in atomic ratios of Cr, Al, and 2Ti. Chromites in other martian meteorites are shown for references. Data source: Floran et al., 1978; Mittlefehldt, 1994; McSween and Jarosewich, 1983; Ikeda, 1994, unpublished data.

Table 2. The average compositions of groundmass (Gdm), groundmass-glass (Gdm-glass), inclusion glass (Inc.-glass) and shock-melt glass in Y980459 shergottite. The bulk composition of the meteorite is shown for reference.

	Gdm	Gdm-glass	Inc.-glass	Shock-melt glass	Bulk
SiO_2	49.64	52.09	62.15	48.39	48.70
TiO_2	1.08	1.17	0.92	0.28	0.54
Al_2O_3	14.76	17.02	11.49	4.04	5.27
Cr_2O_3	0.00	0.03	0.14	0.95	0.71
FeO	18.30	13.92	6.68	18.26	17.32
MnO	0.40	0.26	0.19	0.32	0.52
MgO	1.59	0.72	2.47	20.15	19.62
CaO	9.22	9.72	13.18	5.48	6.37
Na_2O	2.58	2.66	1.34	0.54	0.48
K_2O	0.02	0.06	0.06	0.00	<0.02
P_2O_5	0.79	1.25	0.58	0.01	0.29
FeS					0.26
Total	98.44	98.93	99.18	98.43	99.80
mg	0.134	0.085	0.40	0.06	0.67

The groundmass compositions were obtained by using a broad beam method of an electron-probe micro-analyzer (EPMA).
The glass compositions were obtained by using a focused beam of an EPMA.
The bulk composition was quoted from Misawa (2003).

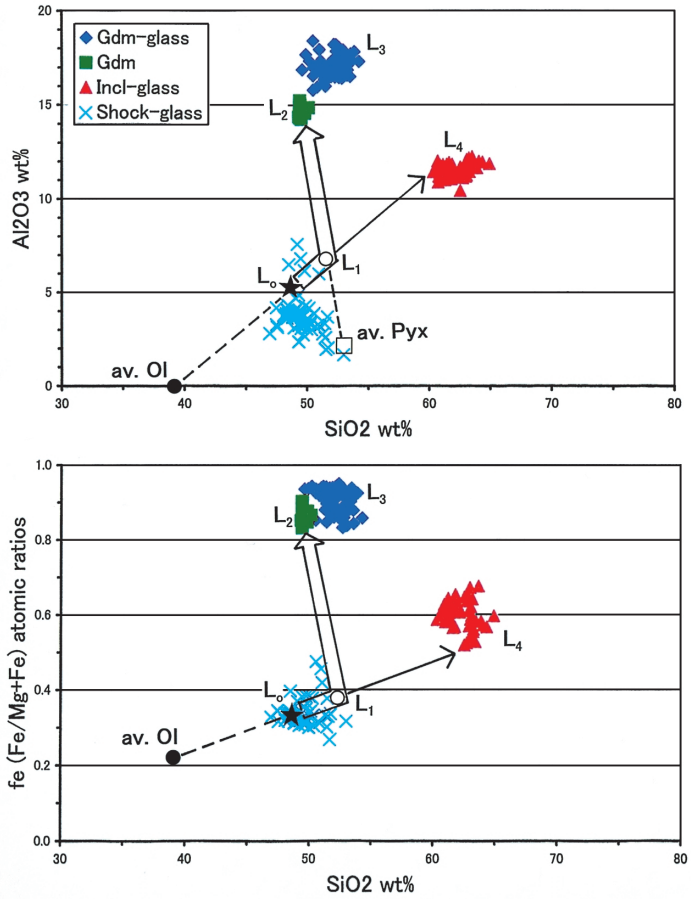

Fig. 7. The Al_2O_3 contents and fe atomic ratios of the groundmass and glass in Y980459 are plotted against their SiO_2 wt%. L_0, L_1, L_2, L_3, and L_4, are bulk of the meteorite, calculated middle-stage melt (see text), the bulk groundmass, groundmass glass, and magmatic inclusion glass, respectively. The shock-glass is shown by blue crosses. The average olivine and pyroxene are shown by av.Ol and av.Pyx, respectively. The fractional crystallization trend for the Y980459 lithology is shown by a broad arrow, and the metastable crystallization trend for magmatic inclusions is shown by a solid line arrow.

the modal composition of orthopyroxene and augite is about 2 : 1, the averaged pyroxene was calculated from averaged compositions of orthopyroxene and augite in the ratio.

Figure 5 shows minor components (Al_2O_3, Cr_2O_3, TiO_2) of pyroxenes in Y980459, where halos in shock melt pockets (see later Section 5.4) are shown together. The Al_2O_3 contents of pyroxenes increase from 0.2 wt% up to 10 wt% in proportion to their fe ratios from 0.17 to 0.77 (Fig. 5). The Cr_2O_3 contents of pyroxenes decrease from 0.9 wt% to less than 0.05 wt%. The TiO_2 contents increase from less than 0.05 wt% up to 2.5 wt% in proportion to their fe ratios.

4.3. Chromite

Chromite occurs as an accessory mineral in Y980459. Chromite is poor in TiO_2 and Al_2O_3, but it shows weak chemical zoning from Cr-richer cores to Al-richer rims (Table 1). The chemical compositions of chromites are plotted in Fig. 6, where zoning trends of chromites in other martian meteorites are shown for reference. The chromites in Y980459 are the richest in Cr and correspond to the Cr-rich cores of chromites in other martian meteorites.

4.4. Groundmass glass and quenched minerals

The groundmass of Y980459 consists of glass and quenched minerals. The quenched minerals show needle-like dendritic outlines and fine-grained irregular shapes. They are ferroan olivine (Fo_{35-15}) and Al-rich pyroxenes (augite and pigeonite), respectively. The groundmass glass has an MgO-depleted basaltic composition. The average chemical composition of the groundmass glass is shown in Table 2, where the glass is enriched in plagioclase components and depleted in MgO and Cr_2O_3 components. The glass contains high P_2O_5 contents.

The chemical composition of the bulk groundmass including groundmass glass and quenched minerals was obtained using the broad beam method of EPMA, and the averaged composition is shown in Table 2. The chemical compositions of the bulk groundmass and the groundmass glass are shown in Fig. 7 denoted by L_2 and L_3, respectively. The groundmass glass is enriched in Al_2O_3, Na_2O and CaO, indicating that it contains abundant plagioclase components. The normative composition of the plagioclase components in the averaged groundmass glass is $An_{58.6}Ab_{40.8}Or_{0.6}$.

4.5. Pyrrhotite

Sulfide rarely occurs as pyrrhotite in the groundmass glass of Y980459 (Fig. 1e), and the chemical composition is shown in Table 1.

5. Discussion

5.1. Classification of Y980459

Y980459 is a glassy basaltic rock, which is different in texture from any other known shergottites. It abundantly contains glass in the groundmass. It may have cooled rapidly, and the fractionated melt was quenched as the glassy groundmass. If this meteorite would have cooled more slowly, it would have crystallized labradoritic plagioclase in the groundmass, because the groundmass glass contains abundant plagioclase components. As the groundmass glass contains high P_2O_5 contents, phosphates also would have crystallized in the groundmass.

The bulk chemical composition of Y980459 (Table 2; Misawa, 2003) is similar to those of the DaG476 and SaU 005 Ol-phyric shergottites (Dreibus *et al*., 2003; Shih *et al*., 2003; Shirai and Ebihara, 2003) and the xenolith-bearing EETA79001A basaltic shergottite (McSween and Jarosewich, 1983). Although DaG476 and SaU 005 have doleritic lithology with olivine phenocrysts, Y980459 has a glassy basaltic lithology. The EETA79001A includes harzburgitic xenoliths, but Y980459 is free from xenoliths.

Generally shergottites were classified into two subgroups, lherzolitic and basaltic

(McSween, 1994). The former contains magnesian olivine as a cumulate phase. The basaltic shergottites are considered to represent basaltic magmas with or without cumulus phases. The dichotomy for shergottites has been used by many researchers. Recently a new type of basaltic shergottites with olivine phenocrysts were recovered from hot deserts, and they were classified to be Ol-phyric shergottites (Goodrich, 2002). They consist mainly of pyroxenes and maskelynite with a variable amount of olivine phenocrysts. However, Y980459 consists mainly of olivine and pyroxenes set in the glassy groundmass, and the texture differs from the Ol-phyric shergottites. Therefore we need a new classification of lithological types of shergottites including a glassy basaltic shergottite. As already stated, the chemical data indicate that Y980459 should be classified as a new type of Ol-phyric shergottites. Therefore, the shergottites should be defined to be martian meteorites having glassy basaltic or doleritic lithologies with variable amounts of olivine, pyroxenes and plagioclase-components, and the plagioclase-components contain plagioclase, maskelynite, or plagioclase-component-rich groundmass glass. The new classification for the lithological types of the shergottite group is shown in Table 3.

Table 3. Type-classification of shergottite group.

Subgroup	Lithological type	Meteorites
Lherzolitic shergottite subgroup		(1) ALHA77005 (2) Y793605 (3) LEW88516 (4) GRV9927 (5) NWA1950
Basaltic shergottite subgroup	Ol-free doleritic type	(1) Shergotty (2) Zagami (3) EETA79001B (4) QUE94201 (5) Los Angeles 001, 002 (6) Dhofar 378 (7) NWA480, 1460 (8) NWA1669 (9) NWA856
Ol-phyric shergottite subgroup	Xenolith-bearing doleritic type	(1) EETA79001A (containing Harzburgite)
	Ol-bearing doleritic type	(1) DaG476, 489, 670, 735, 876, 975 (2) SaU005, 008, 051, 060, 090, 094,120, 150 (3) Dhofar 019 (4) NWA1068, 1110, 1775 (5) NWA1195 (6) NWA2046
	Ol-bearing glassy basaltic type	(1) Y980459

Ol: magnesian olivine, except fayalite.
A lherzolitic shergottite (YA1075) is not yet approved by the nomenclature committee of the Meteoritical Society, and is not tabulated here.

Basaltic and Ol-phyric shergottites are classified into four lithological types, olivine-free doleritic, xenolith-bearing doleritic, olivine-bearing doleritic, and olivine-bearing glassy basaltic. All basaltic and Ol-phyric shergottites except Y980459 were holocrystalline with medium-size grains before the maskelynization, and often have ophitic (doleritic) or subophitic (subdoleritic) textures. Therefore, they are classified as a doleritic type. However, Y980459 has a glassy groundmass and does not show a doleritic texture. Therefore, it is classified as a glassy basaltic type.

5.2. Crystallization of Y980459 main lithology

Although olivine phenocrysts in Ol-phyric shergottites can be cumulus phases or xenocrysts (Goodrich, 2003), olivine phenocrysts in Y980459 may be non-cumulus phenocrysts nor xenocrysts. The reasons are as follows. The olivine phenocrysts in Y980459 contain magmatic inclusions in their cores, and the magmatic inclusions represent the early- to middle-stage melt of Y980459 (see next section). The fact suggests that the olivine phenocrysts in Y980459 may not be xenocrysts derived from the martian mantle such as those in EEYA79001A (McSween and Jarosewich, 1983).

If the olivine phenocrysts in Y980459 are non-cumulus phases, the bulk chemical composition (Table 2) may represent the original magma for Y980459. The partition coefficient of Mg-Fe between olivine and melt is 0.33 (Longhi *et al*., 1978), indicating that magnesian olivine of Fo_{86} should crystallize first from the melt having the Y980459 bulk composition. The magnesian olivine Fo_{86} is very similar to the most magnesian olivine (Fo_{85}) in phenocrysts of Y980459, suggesting that all olivine phenocrysts in Y980459 are non-cumulus phases.

The cores of olivine phenocrysts show zoning from Fo_{85} to Fo_{73}, and minor components also show compositional zoning (Fig. 2). Figure 1f shows a sharp contact in a core of an olivine phenocryst between magnesian olivine (Fo_{83-85}) and less magnesian olivine (Fo_{79-80}), indicating that body diffusion of Mg-Fe did not take place in olivine phenocrysts. The ferroan rims of olivine just in contact with the groundmass (Fig. 1e) may have crystallized directly from the groundmass melt. Therefore, the chemical zoning of Mg-Fe and the minor components may have been mainly produced by fractional crystallization. McKay and Mikouchi (2003) discussed two possibilities for origin of magnesian olivine in Y980459, cumulus and non-cumulus origins, and they concluded that further study for the origin of magnesian olivine is required.

The chemical composition of the original magma for Y980459 is taken to be the bulk composition (L_0 in Figs. 7 and 8). The bulk composition of Y980459 is poor in SiO_2 and plotted in the olivine liquidus field of the pseudo-ternary phase diagram of the Quartz-Olivine-Plagioclase system (Fig. 8). The original magma may have crystallized olivine. The chromites in Y980459 are often included in olivine grains, and they may have precipitated along with olivine.

The precipitation of olivine may have changed the original melt (L_0) to SiO_2-richer melt, and the magma reaches the liquidus field boundary between olivine and orthopyroxene. The melt is denoted as L_1, and it begins to crystallize pyroxenes abundantly. Orthopyroxene first crystallized from L_1 melt and followed by augite to form the augite mantles surrounding orthopyroxene cores. The averaged compositions of orthopyroxene, augite and pyroxenes (Table 1) are plotted in Fig. 8. The chemical

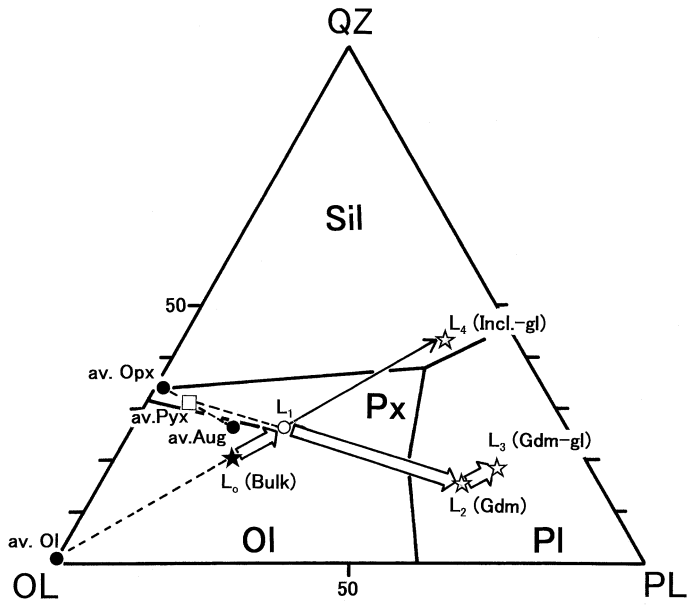

Fig. 8. Crystallization trends of the main lithology of Y980459 and the magmatic inclusions are shown by broad and solid arrows, respectively, in the pseudoternary system of quartz(QZ) -olivine(OL)-plagioclase(PL). The ternary system is projected from wollastonite components in oxygen units. The bold lines are liquidus field boundaries between the two liquidus fields, which are a silica mineral (Sil), pyroxene (Px), olivine (Ol), and plagioclase (Pl) for the melts having an mg ratio of 0.562 and an anorthite molecular ratio of 77, quoted from Longhi and Pan (1989). Averaged orthopyroxene (av.Opx), augite (av.Aug), and olivine (av.Ol) are shown by solid circles, and averaged pyroxene (av.Pyx) is shown by an open square. L_0-L_4: see text.

composition of melt L_1 is obtained as a crossing point of two tie lines, an extension line of olivine and L_0 and a tie line between the averaged pyroxene and the groundmass. The chemical composition of the middle-stage melt is shown in Table 4 and plotted as L_1 in Figs. 7 and 8. The mg ratio of L_1 was taken to be 0.50 (Table 4) so that L_1 can coexist with core olivines of phenocrysts around Fo_{73-74}, which corresponds to the outer parts of the magnesian olivine phenocrysts.

The pyroxenes and minor olivine crystallized from the L_1 melt, and the residual melt became enriched in plagioclase components by their subtraction. The fractionated melt resulted in the groundmass melt (L_2 in Figs. 7 and 8) under rapid cooling condition. During this stage, the rims (Fo_{70-30}) of olivine phenocrysts may have crystallized. Finally, ferroan olivine and pyroxenes crystallized in the groundmass melt under a rapid cooling condition to form quenched crystals. The residual melt changed from L_2 to the most fractionated melt, which was quenched as groundmass glass (L_3 in Figs. 7 and 8). McKay and Mikouchi (2003) suggested that the interstitial melt would be driven deep into the plagioclase stability field by continued crystallization of olivine and pyroxene. Their idea is consistent with the above conclusion. Sulfide occurs in

Table 4. Chemical compositions of calculated middle-stage (less fractionated) magmas (L_1) and the trapped melt (L_T) of magmatic inclusions.

	L_1	L_T
	Calculated*	Calculated**
SiO_2	50.08	51.07
TiO_2	0.67	0.53
Al_2O_3	6.44	6.62
Cr_2O_3	0.79	0.16
FeO	21.01	20.87
MnO	0.54	0.23
MgO	11.79	11.71
CaO	7.73	7.68
Na_2O	0.59	0.77
K_2O	0.02	0.02
P_2O_5	0.35	0.34
Total	100.00	100.00
mg	0.50	0.50

* L_1 is obtained by subtraction of averaged olivine (av.Ol, Table 2) from the whole rock (Table 1) to produce the middle-stage liquid (L_1) which is just on the tie line between the groundmass (Gdm, Table 1) and averaged pyroxene (av.Pyx, Table 2). Finally, the mg atomic ratio of L_1 was revised to be 0.50 so that L_1 can coexist with Fo_{73-74}.

** L_T is obtained by addition of averaged olivine (av.Ol, Table 2) to the magmatic inclusion glass (Table 1) to produce the trapped melt (L_T) in the same way as L_1. Finally, the mg atomic ratio of L_T was revised to be 0.50.

spherical shapes in the groundmass glass, suggesting that they were produced by liquid immiscibility from the surrounding groundmass melt.

The phase relationship of the crystallization trend for Y980459 is well explained by a phase diagram with mg＝0.562 and An＝77 (Longhi and Pan, 1989), as shown in Fig. 8. Especially it is consistent with the phase diagram that L_1 is just on liquidus phase boundary between olivine and low-Ca pyroxene.

5.3. Crystallization of magmatic inclusions

An early- to meddle-stage magma may have been trapped in growing olivine phenocrysts. The trapped melt may have crystallized olivine in the olivine phenocrysts to form the wall olivine surrounding the inclusion melt. The inclusion melt crystallized too much wall olivine under a meta-stable condition, the residual melt became enriched in SiO_2 and plagioclase components, and it was finally quenched as glass in the phenocrysts. The inclusion glass is denoted as L_4 and shown in Figs. 7 and 8, and the average chemical composition of glass is shown in Table 2. The inclusion glass is enriched in both SiO_2 and plagioclase components, and it is more magnesian than the groundmass glass.

An middle-stage melt, for example L_1 in Figs. 7 and 8, can be trapped in olivine

phenocrysts, and it metastably crystallizes wall olivine to change the trapped melt from L_1 to SiO_2-rich melt, which may be quenched as the inclusion glass (L_4). Reversely, wall olivine ($Fo_{\sim 74}$) is added to L_4 to produce the trapped middle-stage magma until the melt comes to the tie line between averaged pyroxene and the groundmass (Fig. 8). The obtained trapped melt is shown in Table 4 as L_T, and is very similar to L_1 (Table 4). The truly-trapped melt can be an early-stage melt between L_0 and L_T (or L_1) in Fig. 8, but it should be near to L_T, because the magmatic inclusions in Y980459 are included in $Fo_{\sim 74}$, suggesting that the truly-trapped melt represent the middle-stage melt and should be near the boundary between olivine and orthopyroxene liquidus fields around L_1.

5.4. Impact shock

Shock-melt pockets in Y980459 consist of shock-melt glass, relic orthopyroxene, relic olivine, and relic chromite (Fig. 1k). The chemical compositions of the shock-melt glass are plotted in Fig. 7, which are similar to the bulk chemical composition of Y980459 (L_0). The relic orthopyroxene grains are always surrounded by halos (Fig. 1l). The width of the halos are about 10μm, and their chemical compositions are similar to that of orthopyroxene with minor shock-melt glass, suggesting that the halos were produced by orthopyroxene needles and minor interstitial shock-melt glass. The orthopyroxene needles may have grown epitaxially on relic orthopyroxene grains under a rapid cooling condition.

Some olivine grains in Y980459 show planar or irregular fractures with undulatory extinction. In addition to these, incipient formation of shock-melt pockets indicates that the degree of impact shock, which was defined for ordinary chondrites (Stöffler *et al.*, 1991), corresponds to S3 for Y980459. Greshake *et al.* (2003) concluded an equi-

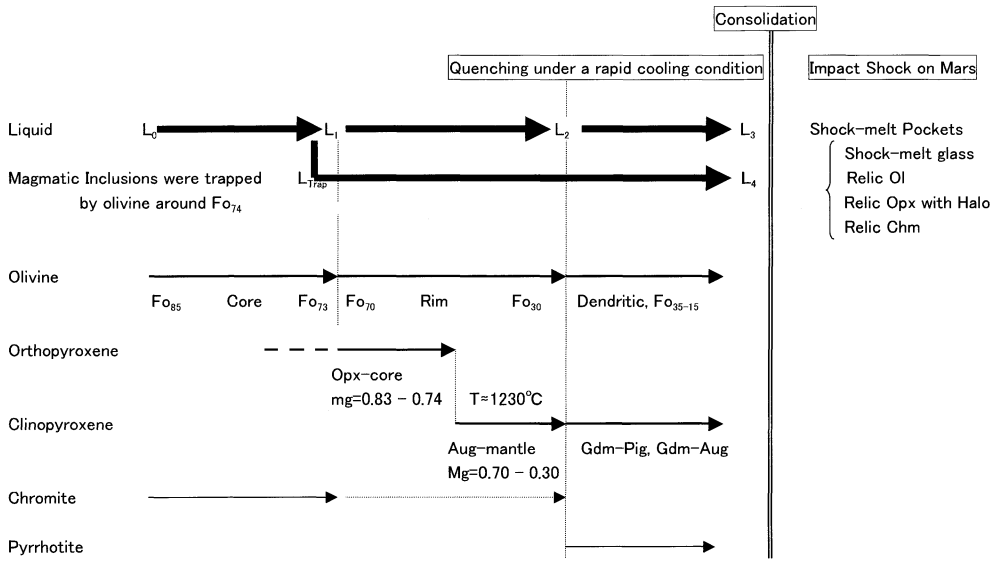

Fig. 9. Crystallization sequence of the Y980459 basaltic shergottite.

librium peak shock pressure of 20–25 GPa for Y980459, and this is consistent with S3.

5.5. *Summary*

The crystallization sequence for Y980459 is summarized in Fig. 9. The original magma is denoted by L_0 in the figure and changed to middle-stage melt (L_1) by crystallization of olivine and further to the fractionated melt (the groundmass melt, L_2) by crystallization of olivine and pyroxenes. The cores of olivine phenocrysts are zoned from Fo_{85} to Fo_{73}, and the rims from Fo_{70} to Fo_{30}. The magmatic inclusions occur in olivine phenocrysts and the olivines just in contact with magmatic inclusions are around Fo_{74}. Therefore, magmatic inclusions may have been trapped just before the crystallization of the rims of olivine phenocrysts. Metastable crystallization of wall olivine in magmatic inclusions changed the trapped melt (L_T) to the SiO_2-rich melt (L_4 in Fig. 9).

Orthopyroxene begins to crystallize from melts around L_1 and is followed by augite mantles. The two pyroxene geothermometer (Lindsley and Andersen, 1983) for pairs of orthopyroxene and augite, which are just in contact with each other, gives the equilibrium temperature of about 1230°C. The groundmass melt L_2 finally crystallized dendritic ferroan olivine and fine-grained groundmass pyroxene grains under a rapid cooling condition. The final residual melt quenched as glass of L_3. Sulfide melt spherules may have produced by liquid immiscibility from melts between L_2 and L_3, and the sulfide spherules precipitated pyrrhotite in them. The rapid cooling for Y980459 suggests that it was a lava flow on Mars. After the consolidation, an impact shock took place on Mars, producing shock-melt pockets in Y980459.

6. Conclusions

1) Y980459 is a new type of Ol-phyric shergottites. It consists of olivine, orthopyroxene with augite mantles, chromite, sulfide with glassy groundmass. There is neither plagioclase nor maskelynite. It may have cooled rapidly at a surficial zone of a lava flow on Mars.

2) Classification of lithological types for the basaltic shergottites was proposed, and Y980459 is classified as an olivine-bearing glassy basaltic type.

3) Phenocrystic olivine ranges in mg ratios from 0.85 to 0.73. The olivine with mg of 0.85 is the most magnesian among all martian meteorites.

4) Orthopyroxene occurs in cores of pyroxene grains and ranges in mg from 0.83 to 0.74. Pyroxene grains are always surrounded by augite mantles ranging in mg from 0.7 to 0.3.

5) Chromite has less-fractionated compositions than any other martian meteorites.

6) Magmatic inclusions occur in olivine grains, and they are mostly pure glass. Trapped melt (L_T) was estimated from magmatic inclusions by addition of the wall olivine, and it is very similar to the middle-stage melt (L_1) of the Y980459 crystallization sequence.

7) Shock-melt pockets are observed, and the shock degree of Y980459 corresponds to S3.

Acknowledgments

I thank the NIPR for renting of sample, and Dr. Misawa for the consortium study of Y980459. I also thank Dr. Mikouchi and an anonymous referee for their constructive reviews.

References

Bunch, T.E. and Reid, A.M. (1975): The nakhlites Part I: Petrography and mineral chemistry. Meteoritics, **10**, 303–315.

Floran, R.J., Prinz, M., Hlava, P., Keil, K., Nehru, C.E. and Hinthorne, J. (1978): The Chassigny meteorite: A cumulus dunite with hydrous amphibole-bearing melt inclusions. Geochim. Cosmochim. Acta, **42**, 1213–1229.

Dreibus, G., Haubold, R., Huisl, W. and Spettel, B. (2003): Composition of the chemistry of Yamato 980459 with DaG476 and SaU 005. International Symposium—Evolution of Solar System Materials: A New Perspective from Antarctic Meteorites. Tokyo, Natl Inst. Polar Res., 19–20.

Goodrich, C.A. (2002): Olivine-phyric martian basalts: A new type of shergottite. Meteorit. Planet. Sci., **37**, B31–B34.

Goodrich, C.A. (2003): Petrogenesis of olivine-phyric shergottites Sayh al Uhaymir 005 and Elephant Moraine A79001 lithology A. Geochim. Cosmochim. Acta, **67**, 3735–3772.

Greshake, A., Fritz, J. and Stöffler, D. (2003): Petrography and shock metamorphism of the unique shergottite Yamato 980459. International Symposium—Evolution of Solar System Materials: A New Perspective from Antarctic Meteorites. Tokyo, Natl Inst. Polar Res., 29–30.

Hale, V.P.S., McSween, H.Y. and McKay, G. (1999): Re-evaluation of intercumulus liquid composition and oxidation state for the Shergotty meteorite. Geochim. Cosmochim. Acta, **63**, 1459–1470.

Harvey, R. and McSween, H.Y. (1992): The parent magmas of the nakhlite meteorites: Clues from melt inclusions. Earth Planet. Sci. Lett., **111**, 467–482.

Harvey, R.P. and McSween, H.Y. (1994): Ancestor's bones and palimpsests: Olivine in ALH84001 and orthopyroxene in Chassigny (abstract). Meteoritics, **29**, 472.

Ikeda, Y. (1994): Petrography and petrology of the ALH77005 shergottite. Proc. NIPR Symp. Antarct. Meteorites, **7**, 9–29.

Ikeda, Y. (1997): Petrology and mineralogy of the Y-793605 Martian meteorite. Antarct. Meteorite Res., **10**, 13–40.

Ikeda, Y. (1998): Petrology of magmatic silicate inclusions in the Allan Hills 77005 lherzolitic shergottite. Meteorit. Planet. Sci., **33**, 803–812.

Ikeda, Y., Takeda, H., Kimura, M. and Nakamura, N. (2002): A new shergottite, Dhofar 378 (abstract). Antarctic Meteorites XXVII. Tokyo, Natl Inst. Polar Res., 40–42.

Imae, N., Ikeda, Y., Shinoda, K., Kojima, H. and Iwata, N. (2003): Yamato nakhlites: Petrology and mineralogy. Antarct. Meteorite Res., **16**, 13–33.

Kojima, H. and Imae, N. (2002): Meteorite Newslett., **11** (1), 45.

Lindsley, D.H. and Andersen, D.J. (1983): A two-pyroxene thermometer. Proc. Lunar Planet. Sci. Conf., 13th, Part 2, A887–A906 (J. Geophys. Res., **88** Suppl.).

Longhi, J., Walker, D. and Hays, J.F. (1978): Fe and Mg distribution between olivine and lunar basaltic liquids. Geochim. Cosmochim. Acta, **42**, 1545–1558.

Longhi, J. and Pan, V. (1989): The parent magmas of the SNC meteorites. Proc. Lunar Planet. Sci. Conf., 19th, 451–464.

McKay, G. and Mikouchi, T. (2003): Crystallization of Antarctic shergottite Yamato 980459. International Symposium—Evolution of Solar System Materials: A New Perspective from Antarctic Meteorites. Tokyo, Natl Inst. Polar Res., 76–77.

McSween, H.Y. (1994): What we have learned about Mars from SNC meteorites. Meteoritics, **29**, 757–779.

McSween, H.Y. and Jarosewich, E. (1983): Petrogenesis of the Elephant Moraine A79001 meteorite: Multiple magma pulses on the shergottite parent body. Geochim. Cosmochim. Acta, **47**, 1501–1513.

Mikouchi, T. and Miyamoto, M. (2002): Mineralogy and olivine cooling rate of the Dhofar 019 shergottite. Antarct. Meteorite Res., **15**, 122–142.

Mikouchi, T., Koizumi, E., McKay, G., Monkawa, A., Ueda, Y. and Miyamoto, M. (2003): Mineralogy and petrology of the Yamato 980459 martian meteorite: A new shergottite-related rock. International Symposium—Evolution of Solar System Materials: A New Perspective from Antarctic Meteorites. Tokyo, Natl Inst. Polar Res., 82–83.

Misawa, K. (2003): The Yamato 980459 shergottite consortium. International Symposium—Evolution of Solar System Materials: A New Perspective from Antarctic Meteorites. Tokyo, Natl Inst. Polar Res., 84–85.

Mittlefehldt, D.W. (1994): ALH84001, a cumulate orthopyroxenite member of the martian meteorite clan. Meteoritics, **29**, 214–221.

Russell, S., Ziphel, J., Grossman, J.N. and Grady, M.M. (2002): The Meteoritical Bulletin, No. 86, 2002 July. Meteorit. Planet. Sci., **37** (Suppl.), A157–A184.

Russell, S., Ziphel, J., Folco, L., Jones, R., Grady, M.M., McCoy, T. and Grossman, J.N. (2003): The Meteoritical Bulletin, No. 87, 2003 July. Meteorit. Planet. Sci., **38** (Suppl.), A189–A248.

Sautter, V., Barrat, J.A., Jambon, A., Lorand, J.P., Gillet, P., Javoy, M., Jaron, J.L. and Lesourd, M. (2002): A new Martian meteorite from Morocco: the nakhlites North West Africa 817. Earth Planet. Sci. Lett., **195**, 223–238.

Shih, C.-Y., Nyquist, L.E. and Wiesmann, H. (2003): Isotopic studies of Antarctic olivine-phyric shergottite Y980459. International Symposium—Evolution of Solar System Materials: A New Perspective from Antarctic Meteorites. Tokyo, Natl Inst. Polar Res., 125–126.

Shirai, N. and Ebihara, M. (2003): Chemical composition of Yamato 980459. International Symposium—Evolution of Solar System Materials: A New Perspective from Antarctic Meteorites. Tokyo, Natl Inst. Polar Res., 127–128.

Stöffler, D. (2000): Maskelynite confirmed as diaplectic glass: Indication for peak shock pressures below 45 GPa in all martian meteorites. Lunar and Planetary Science XXXI. Houston, Lunar Planet. Inst., Abstract #1170 (CD-ROM).

Stöffler, D., Keil, K. and Scott, E.R. (1991): Shock metamorphism of ordinary chondrites. Geochim. Cosmochim. Acta, **55**, 3845–3867.

Treiman, A. (1985): Amphibole and hercynite spinel in Shergotty and Zagami: Magmatic water, depth of crystallization and metasomatism. Meteoritics, **20**, 227–242.

Treiman, A.H., McKay, G.A., Bogard, D.D., Mittlefehldt, D.W., Wang, M.S., Keller, L., Lipschutz, M.E., Lindstrom, M. and Garrison, D. (1994): Comparison of the LEW88516 and ALHA77005 Martian meteorites: Similar but distinct. Meteoritics, **29**, 581–582.